AFM imaging and plasmonic detection of organic thin-films deposited on nanoantenna arrays

Paul, Jharna; McMeekin, Scott G.; De La Rue, Richard M.; Johnson, Nigel P.

Published in:
Sensors and Actuators A: Physical

DOI:
10.1016/j.sna.2018.05.032

Publication date:
2018

Document Version
Publisher's PDF, also known as Version of record

Sensors and Actuators A 279 (2018) 36–45

Contents lists available at ScienceDirect

Sensors and Actuators A: Physical

journal homepage: www.elsevier.com/locate/sna

AFM imaging and plasmonic detection of organic thin-films deposited on nanoantenna arrays

Jharna Paul[a,*], Scott G. McMeekin[b], Richard M. De La Rue[a], Nigel P. Johnson[a]

[a] Division of Electronics and Nanoscale Engineering, School of Engineering, University of Glasgow, Glasgow, G12 8LT, United Kingdom
[b] School of Engineering and Built Environment, Glasgow Caledonian University, Glasgow, G4 0BA, United Kingdom

ARTICLE INFO

Article history:
Received 20 December 2017
Received in revised form 10 May 2018
Accepted 18 May 2018
Available online 24 May 2018

Keywords:
Organic molecules
Plasmonic nanoantennas
AFM imaging
Spectroscopy and sensing

ABSTRACT

In this study, atomic force microscopy (AFM) imaging has been used to reveal the preferential deposition of organic thin-films on patterned nanoantenna array surfaces - identifying the localised formation of both monolayer and multilayer films of octadecanethiol (ODT) molecules, depending on the concentration of the solutions used. Reliable identification of this selective deposition process has been demonstrated for the first time, to our knowledge. Organic thin-films, in particular films of ODT molecules, were deposited on plasmonic resonator surfaces through a chemi-sorption process - using different solution concentrations and immersion times. The nanoantennas based on gold asymmetric-split ring resonator (A-SRR) geometries were fabricated on zinc selenide (ZnSe) substrates using electron-beam lithography and the lift-off technique. Use of the plasmonic resonant-coupling technique has enabled the detection of ODT molecules deposited from a dilute, micromolar (1 μM) solution concentration - with attomole sensitivity of deposited material per A-SRR – a value that is three orders of magnitude lower in concentration than previously reported. Additionally, on resonance, the amplitude of the molecular vibrational resonance peaks is typically an order of magnitude larger than that for the non-resonant coupling. Fourier-transform infrared (FTIR) spectroscopy shows molecule specific spectral responses – with magnitudes corresponding to the different film thicknesses deposited on the resonator surfaces. The experimental results are supported by numerical simulation.

1. Introduction

The spatially localised deposition of organic thin-films on plasmonic nanoantenna arrays is promising, due to the potential of such arrays in offering a suitable interfacial platform for selective binding of biomolecules and nanoparticles over a wide range of sensing applications, e.g. in the recognition of biomolecules and in cell-culture research [1–4]. With the advances in imaging technologies such as atomic force microscopy (AFM), the specific deposition nature of organic thin-films on patterned nanoantenna array surfaces can be further revealed. Organic thin-films - in particular films of octadecanethiol (SH $(CH_2)_{17}$ CH_3), which was chosen as an analyte molecule because it is an important linker molecule with a longer-chain methyl (CH_3) terminal group - produce hydrophobic-film surfaces that have reduced free-energy and surface contamination. Such films produce functionalised surfaces that are suitable for further binding of biomolecules and nanoparticles for bio-medical and environmental applications - and their interaction with plasmonic nanoantennas. The formation of thin-films from octadecanethiol (ODT) molecules on gold surfaces through a chemisorption process is mainly driven by the molecular self-assembly of energetic covalent bonding between active sulphur and gold (S-Au) atoms. Together with the van der Waals interaction between the alkyl chain lengths, self-assembly determines the packing density - and the terminal group defines the functionality of the assembled films [5,6].

The deposited material may form mono- or multi-layer films – depending on various parameters, such as the assembly procedure, the solution concentration, the immersion time and the nature of the solvents used [5,7,8]. The thickness of a complete monolayer-film is approximately 2.4 nm [9], which is also the theoretical length of an ODT molecule.

The adsorption of thiols on planar-gold substrates has been imaged using several different microscopy techniques [10,11]. However, no direct imaging has been reported in studies of the specific deposition nature of organic molecular films on the patterned plasmonic nanoantenna array surfaces. Regardless, plasmonic nanoantennas are subwavelength structures that interact

* Corresponding author.
E-mail address: Jharna.Paul@glasgow.ac.uk (J. Paul).

https://doi.org/10.1016/j.sna.2018.05.032

with light and subsequently give rise to localised and resonant-enhancement of the optical intensity within a very small volume [12–14]. This enhancement facilitates the excitation of the molecular bond vibrations of thin-films deposited on the resonator surfaces, with enhanced sensitivity of detection [1–3,9,15–26]. The plasmonic resonances of engineered nanoantenna arrays depend on their structural geometries and the surrounding dielectric environments – providing the opportunity to tune the resonances to match with those of the targeted molecular bond vibrations of interest. This enables the amplification of inherently weak molecular signals, through surface enhanced infrared absorption (SEIRA) spectroscopy, for detection of deposited-films on resonator surfaces from dilute solution concentrations. The plasmonic resonant coupling approach is based on the well-known SEIRA technique – and has been widely reported in the literature [9,15,16,18,19,23] for detection of small numbers of moderate size organic molecules. ODT, with a molecular weight (MW) of 286.56 g/mol [27], has been found to provide a useful model molecule that is comparable in size with important biomolecules, such as the hormone 17β estradiol with a MW of 272.382 g/mol [20]. ODT has therefore been used for characterisation in bio-medical and environmental monitoring applications. Additionally, the shift in the plasmonic resonance position due to the change in refractive index caused by ODT molecular binding has been reported by Chen et al. [23]. The ODT molecules have the strongest IR active anti-symmetric and symmetric CH_2 stretching vibrational modes at wavelengths around 3.41 to 3.43 μm (2936 to 2916 cm^{-1}) and 3.493 to 3.51 microns (2863 to 2850 cm^{-1}), respectively [28].

Furthermore, asymmetric-split ring resonator (A-SRR) based nanoantennas are characteristically capable of producing sharper responses with multiple plasmonic resonances [29–31] - due to their different arc lengths, as compared with symmetric split-ring resonators (SRRs) [15]. The inherent fingerprints of many organic molecules appear in the mid-infrared (mid-IR) wavelength regions, e.g. the ODT molecules studied in this work and in the literature [9,15,16,18,19,23], poly-methyl methacrylate (PMMA) [22,31–33], and various proteins [1–3,25] - making the plasmonic-nanoantenna array based sensor a promising candidate for mid-IR sensing applications.

The SEIRA technique based on plasmonic-resonant coupling for enhancement of the sensitivity of detection of ODT molecules was first reported by Nubrech et al. [9], followed by Cubukcu et al. [15] - and more recently by several groups of researchers [16,18,19,23]. The SEIRA approach has been widely studied and has shown promise for a broad range of applications in bio-medical and environmental monitoring. Since the ODT molecule is a well-known model and an important linker molecule that provides a functionalised surface for further binding of bio-molecules and nanoparticles, identification of the exact deposition nature of the ODT molecules on patterned nanoantenna array surfaces is crucial, in combination with an accurate estimation of the formation of monolayer vs multilayer films of ODT molecules deposited on the resonator surfaces using different solution concentrations.

In this study, we report the use of AFM imaging to investigate the selective deposition nature of ODT molecular thin-films on patterned nanoantenna array surfaces – clearly revealing the localised formation of both monolayer and multilayer films of octadecanethiol (ODT) molecules, depending on the concentration of the solutions used, in conjunction with Fourier-transform infrared (FTIR) spectroscopy for molecular vibrational detection. Thin-films on gold A-SRR surfaces are formed through the molecular self-assembly procedure - using micromolar (1 μM) and millimolar (2.5 mM) solution concentrations of ODT molecules, with continuous immersion times of 24 and 3 h respectively. We examine, in particular, how the thicknesses and the nature of the deposition of these films vary with the experimental conditions. FTIR spectroscopy has been used to excite the vibrational ODT molecular signal, under both plasmonic resonant and non-resonant coupling conditions. The resonant-coupling enables the detection of the dilute, micromolar (1 μM) solution concentration with a monolayer film formation onto the resonator surfaces. Furthermore, gold A-SRRs were fabricated on zinc selenide (ZnSe) substrates purchased from Crystran [34] - using electron-beam lithography (EBL) and lift-off, because ZnSe is highly transparent throughout both the visible and near-to-mid infrared regions, unlike the fused silica that is more commonly used.

2. Materials and methods

The asymmetric-split ring resonators (A-SRRs) were modelled using a commercial finite-difference time domain (FDTD) Lumerical software package. Details regarding the modelling and fabrication of A-SRRs, deposition of organic thin-films, FTIR measurements and AFM imaging techniques are available in the supporting document.

3. Results

The A-SRRs had a circular basic geometry and consisted of two different and opposite arcs separated by identical gaps of 26° arc-sectors (φ (= 16°) is the angle of the asymmetry) and, with a strip width (w) of 100 nm, were realised on a ZnSe substrate. The same design was used for all the fabricated A-SRR array patterns, via L-edit software. A schematic representation of the ASRR pattern is shown in Fig. 1(a), where d is the outer ring diameter. A-SRRs with outer ring diameters (d) of 710 nm, 730 nm, 750 nm, and 1180 nm were used in this work.

All transmittance spectra were measured at normal incidence using an FTIR spectrometer i.e. with the incident electric field (E) excited parallel to the Y-axis direction, as in Fig. 1(a). The measured transmittance spectra for the 730 nm diameter A-SRR arrays (red-colour), together with the simulation spectra (green-colour in the on-line version), are shown in Fig. 1(b), where the plasmonic responses were found to appear within the 3–5 μm wavelength spectral region.

3.1. Resonant-coupling

Following the characterisation of the A-SRRs, continuous formation of the 1 μM solution concentration ODT molecular-film was performed on the gold A-SRR array surfaces, for an immersion time of 24 h. The shorter wavelength transmission minimum in the plasmonic responses of the 730 nm diameter A-SRR array was found to match well with the CH_2 stretching vibrations of the ODT molecules, as shown in Fig. 2 - over the narrow spectral range around a wavelength of 3.5 μm, with an experimental measurement area of 300 × 300 μm^2. The two dotted vertical lines highlight the position of the ODT molecular absorption peak, in relation to the rest of the spectrum. Even for the resonant coupling condition, the vibrational signal from the adsorbed ODT thin-film is hardly discernible (over the spectral range from 2.5 to 5.5 μm). When the spectra were magnified specifically over the range from 3.3 to 3.6 μm, the symmetric CH_2 stretching vibrational mode of the ODT molecules at 3.5 μm (corresponding to 2857 cm^{-1} in wavenumber) became quite prominent - as shown in the inset of Fig. 2.

Fig. 3(a) and (b) show the 2-D AFM images of the 730 nm diameter gold A-SRR arrays, with and without deposition of the 1 μM solution ODT molecular film on their surfaces respectively - over an area of 10 × 10 μm^2. The insets show an expanded view of the same images. In order to find the thickness of the deposited film, the images in Fig. 3(a) and (b) were manually cross-sectioned to show

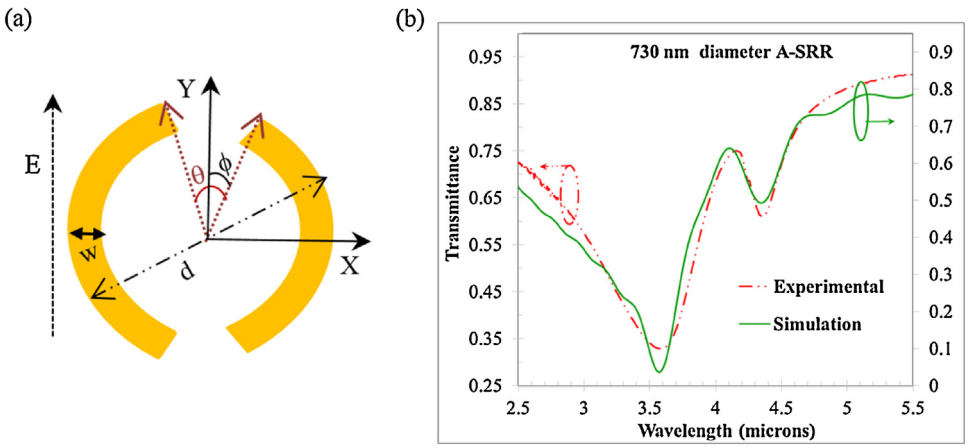

Fig. 1. (a) Schematic of an A-SRR with outer ring diameter, d (710, 730, 750, 1180 nm used in this work) and gap angle of $\theta = 26^{\circ}$, φ ($= 16^{\circ}$) is the angle of the asymmetry and the strip width, $w = 100$ nm and gold thickness (100 nm) was kept constant for all the A-SRR designs in L-edit and are realised on ZnSe substrate (Diagram drawn not to scale). The incident light electric field (E) is excited parallel to the Y-axis direction. (b) Comparison between the experimental and simulation data of the 730 nm diameter A-SRR arrays.

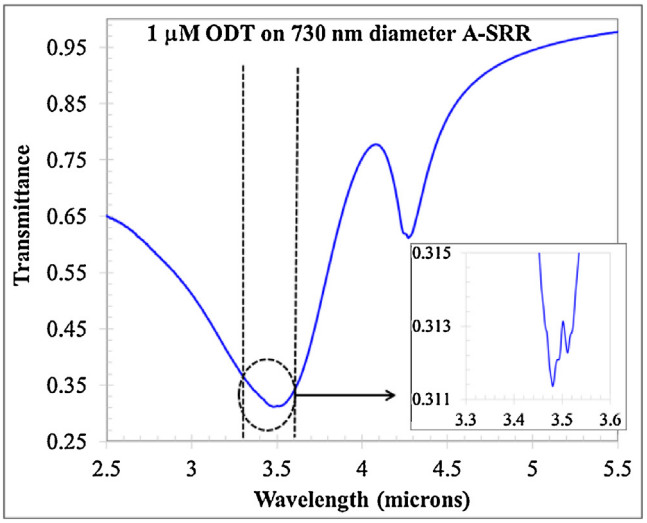

Fig. 2. Transmittance spectral response of the 1 μM solution concentration of ODT molecular-film on the 730 nm diameter ASRR array surfaces, where the dotted vertical lines show the position of the ODT adsorption peak relative to the rest of the spectrum. The inset shows the magnified spectrum of the symmetric vibrational resonance of ODT molecules over the 3.3–3.6 μm spectral region.

the small amplitude difference in the height profiles, in Fig. 4(a) and (b). Although the offsets of the traces in Fig. 4(a) and (b) are different, the calculation of the height difference is based on an average of 6 rows and fourteen arcs of the A-SRRs. From the AFM data, the average thickness of the adsorbed 1 μM solution concentration ODT molecules was found to be 2.34(±0.1) nm and was calculated from the difference between the average height of the A-SRRs with ODT molecules deposited on them - and the height of the ASRRs alone. This value corresponds to monolayer formation of the ODT-film being deposited on the ASRR array surfaces – with a thickness of approximately 2.4 nm [9]. Based on the images and the scan profiles, we conclude that, for the dilute (1 μM) ODT solution concentration, the deposited ODT molecules are mostly attached to the A-SRR surfaces.

Based on the estimated surface packing density of the ODT molecules, 0.222 nm^2/molecule [15], the number of adsorbed ODT molecules on the surface area (total arc surface areas plus edge regions) of a single A-SRR is estimated to be approximately 9.4×10^5 molecules, corresponding to approximately 1.6 amol. Using the measured thickness of 2.34 nm and the density of the ODT molecules of 0.847 g/ml [27], the mass (density × volume) of the molecules deposited on the volume (total area × measured thickness) of an A-SRR was found to be 4.15×10^{-16} g, resulting in the estimated number of adsorbed molecules per A-SRR being approximately 8.7×10^5 molecules, corresponding to approxi-

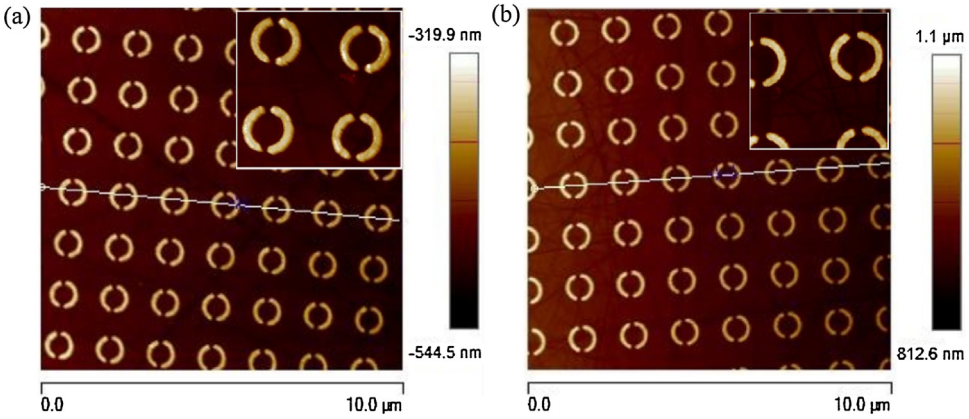

Fig. 3. 2-D AFM images of the 730 nm diameter ASRR arrays: (a) with - and (b) without 1 μM solution concentration of ODT molecular film-deposition on their surfaces, over an area of 10×10 μm^2. The insets show expanded views of the same image respectively.

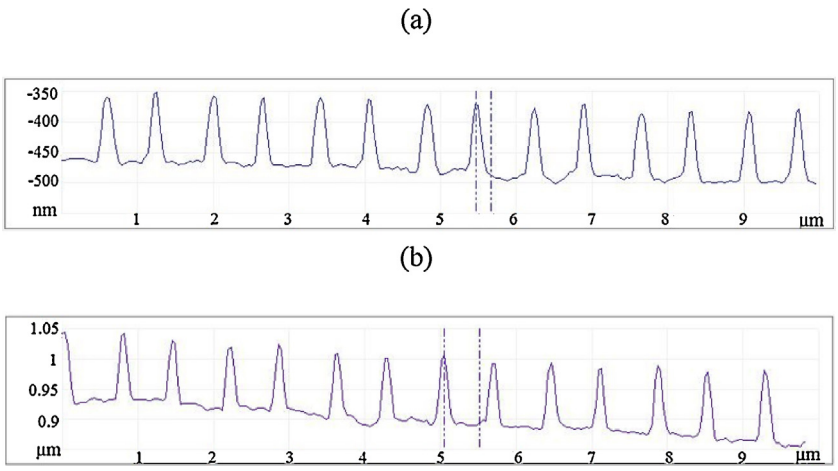

Fig. 4. (a) and (b) Height profiles of cross-sections of the AFM images in Fig. 3(a) and (b) respectively.

Table 1
The number of adsorbed ODT molecules deposited from a 1 μM solution concentration on an A-SRR and on the total number of A-SRRs over a measured area of 300 × 300 μm^2.

Area-based					
A-SRR diameter (nm)	Total A-SRRs (300 × 300 μm^2)	ODT Packing density (nm^2/molecule)	Area of an A-SRR (nm^2)	Molecules adsorbed per A-SRR	Molecules adsorbed on total A-SRRs
730	42,222	0.222	209332	9.4×10^5 molecules 1.57×10^{-18} moles (1.6 attomole)	3.98×10^{10} molecules 6.6×10^{-14} moles (66 femtomole)
Volume-based					
A-SRR diameter (nm)	Total A-SRRs (300 × 300 μm^2)	ODT density (g/m^3)	Volume of an A-SRR (nm^3)	Molecules adsorbed per A-SRR	Molecules adsorbed on total A-SRRs
730	42,222	847000	489837	8.7×10^5 molecules 1.45×10^{-18} moles (1.5 attomole)	3.68×10^{10} molecules 6.1×10^{-14} moles (61 femtomole)

mately 1.5 amol. Detailed calculations on both the area-based and volume-based estimates are given in Table 1.

Further experiments were performed with the higher ODT molecular solution concentration of 2.5 mM, for a 3 h immersion time - using the same continuous self-assembly procedure to deposit the ODT-films on the A-SRR array surfaces as before. For these experiments, arrays with different A-SRRs with outer-ring diameters of 710 nm, 730 nm, 750 nm and 1180 nm were fabricated using the same electron-beam lithography, followed by the lift-off technique. The transmittance spectra of the 710, 730 and 750 nm ASRR arrays alone are shown in Fig. 5(a), over a measurement area of 300 × 300 μm^2.

The molecular vibrational responses from the deposited 2.5 mM solution concentration of ODT molecular-films (only for three hours immersion) on the 730 nm diameter nanoantenna array surfaces are shown in Fig. 5(b) - over the spectral range from 2.5 to 5.5 μm and a measurement area of 300 × 300 μm^2. In this case, both the vibrational peaks from the deposited ODT-films are easily visible (over the wavelength range from 2.5 to 5.5 μm), as compared with the vibrational signal shown in Fig. 2 obtained from the ODT molecular-film deposited from a dilute (1 μM) solution concentration (although immersed for 24 h). Additionally, the inset showing the corresponding magnified spectra with both the anti-symmetric and symmetric ODT vibrational peaks at wavelengths of 3.42 and 3.5 μm (corresponding to 2923.98 and 2857 cm^{-1} wavenumbers) respectively, over the spectral region from 3.3 to 3.6 μm. Similar results were obtained on the 710 and 750 nm diameter A-SRR array surfaces - and are shown in the supplementary document - in Fig. S1(a) and (b), respectively. Fig. 5(c) shows the magnified overlapping spectra from the insets in Figs. 2 and 5(b), respectively, for the adsorbed ODT molecular-films on the resonator array surfaces obtained from 1 μM and 2.5 mM solution concentrations. The symmetric ODT vibrational peak at 3.5 μm from the dilute, 1 μM solution concentration of ODT monolayer-film overlaps closely with the peak from the adsorbed ODT multilayers film obtained from a 2.5 mM solution concentration. For the resonant-coupling condition, it was estimated that the amplitude of the adsorbed ODT symmetric peak is approximately an order of magnitude higher for deposition from a 2.5 mM ODT solution concentration with only 3 h immersion time - as compared with that for the dilute, 1 μM concentration ODT solution deposition, for a 24 h immersion time. This result implies that an order of magnitude greater peak amplitude is achieved by using a three orders of magnitude greater solution concentration (from 1 μM to 2.5 mM) of ODT molecules.

To evaluate the vibrational signal enhancement of the adsorbed ODT-films on plasmonic nanoantenna array surfaces, other experiments were carried out in identical environments where the bare ZnSe substrate was immersed in 2.5 mM concentration solution of ODT molecules, for the same continuous immersion time of 3 h. The spectrum from the adsorbed 2.5 mM solution of ODT molecules on 730 nm diameter A-SRRs, compared with that of the molecules deposited on the bare ZnSe substrate alone, are shown in Fig. 6(a) - over the spectral range from 2.5 to 5.5 μm, with a measurement area of 300 × 300 μm^2. Due to the resonant-plasmonic coupling - the adsorbed ODT molecular vibrational peaks (position indicated by the dotted vertical lines) are easily visible on the nanoantenna arrays, as compared with those of the vibrational signal of the deposited-films on bare substrates alone (which are hardly visible), albeit that identical deposition conditions were used. To compare the strength of the vibrational peaks, both spectra were magnified

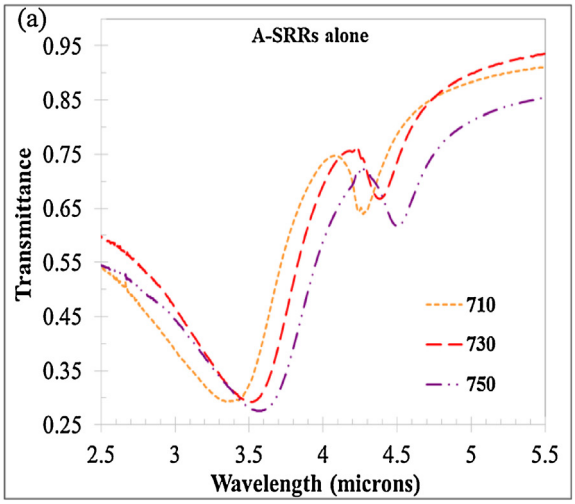

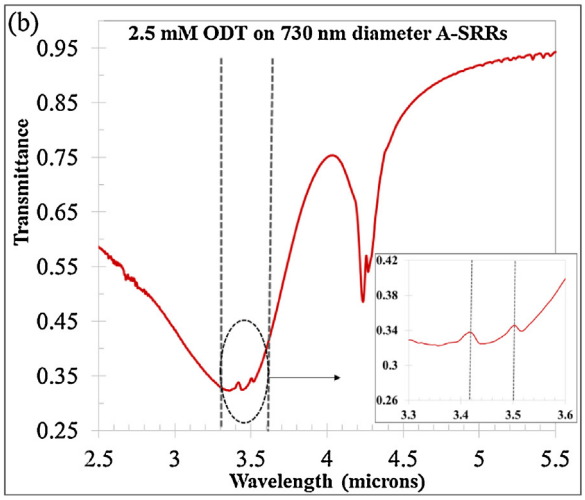

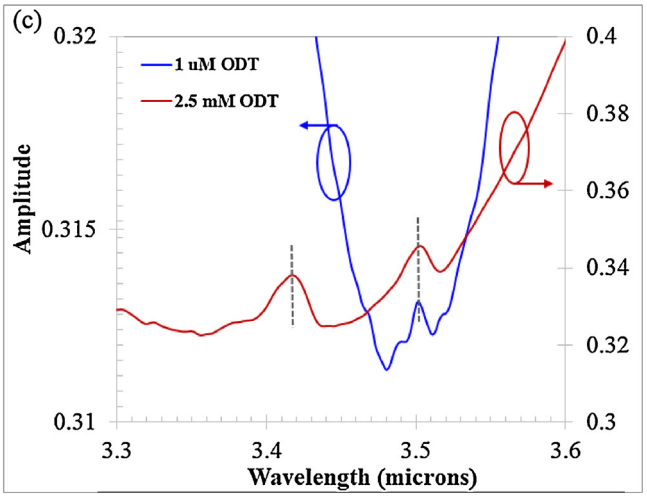

Fig. 5. (a) Transmittance spectra of 710, 730 and 750 nm diameter A-SRR arrays alone. (b) Response of the deposited 2.5 mM solution concentration of ODT molecular-films on 730 nm diameter A-SRR arrays, where the dotted vertical lines show the position of the ODT absorption peaks relative to the rest of the spectra. The inset shows the magnified spectra of both ODT vibrational peaks over the 3.3 to 3.6 μm spectral region. The peak at a wavelength of 4.2 μm indicates the presence of atmospheric carbon dioxide (CO_2). (c) The magnified overlapping spectra from the insets shown in Figs. 2 and 5(b) respectively for the adsorbed 1 μM and 2.5 mM solutions concentration of ODT molecular-films on A-SRR array surfaces.

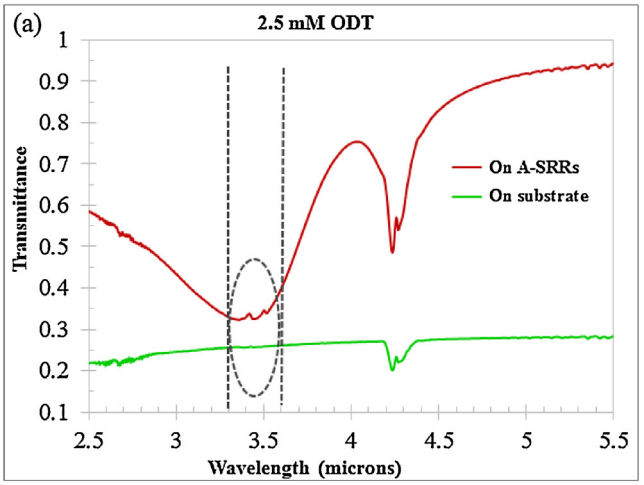

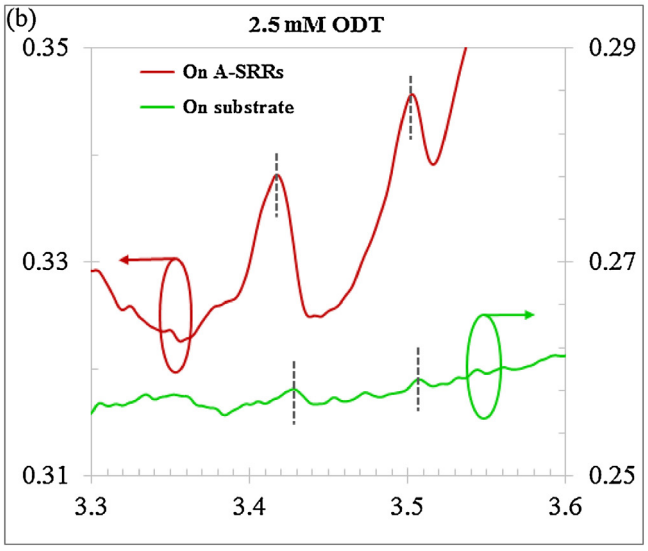

Fig. 6. (a) Comparison spectra of the 2.5 mM solution concentration of ODT molecular-films deposition on 730 nm diameter A-SRR array surface and on bare ZnSe substrate surface, where the dotted vertical lines show the position of the ODT absorption peaks relative to the rest of the spectra. The peak at a wavelength of 4.2 μm indicates the presence of atmospheric carbon dioxide (CO_2). (b) The magnified spectra of both ODT vibrational peaks over the 3.3–3.6 μm spectral region.

over the range from 3.3 to 3.6 μm, and are shown in Fig. 6(b). It is estimated that the change in amplitude of the adsorbed ODT vibrational peaks is approximately ten times smaller for a wavelength at 3.42 μm and approximately thirteen times smaller at 3.5 μm vibrational peak, for the deposition on the bare ZnSe substrate alone as compared with those on the resonant A-SRR array surfaces.

Fig. 7(a) and (b) show the two-dimensional (2-D) AFM images of the ODT molecular-films adsorbed on the 730 nm diameter A-SRR array surfaces from a 2.5 mM solution concentration, over an area of 10×10 μm^2, together with a closer view over 3×3 μm^2, together with the 3-D image is in Fig. 7(c). These images clearly show the formation of inhomogeneous and multilayer ODT-films that are confined almost completely to the surfaces of the ASRR elements in the arrays - but are also, to a limited extent, in the gaps of the A-SRRs (see Fig. 7(b)), together with some molecular deposition on the substrate surfaces.

The auto-generated scan profile obtained during the build-up of the AFM image (in Fig. 7(a)) is shown in Fig. 8(a) where the non-uniformity in the deposited film thicknesses is clearly visible. The height profiles of cross-sections of the images in Fig. 7(a) and (b) are

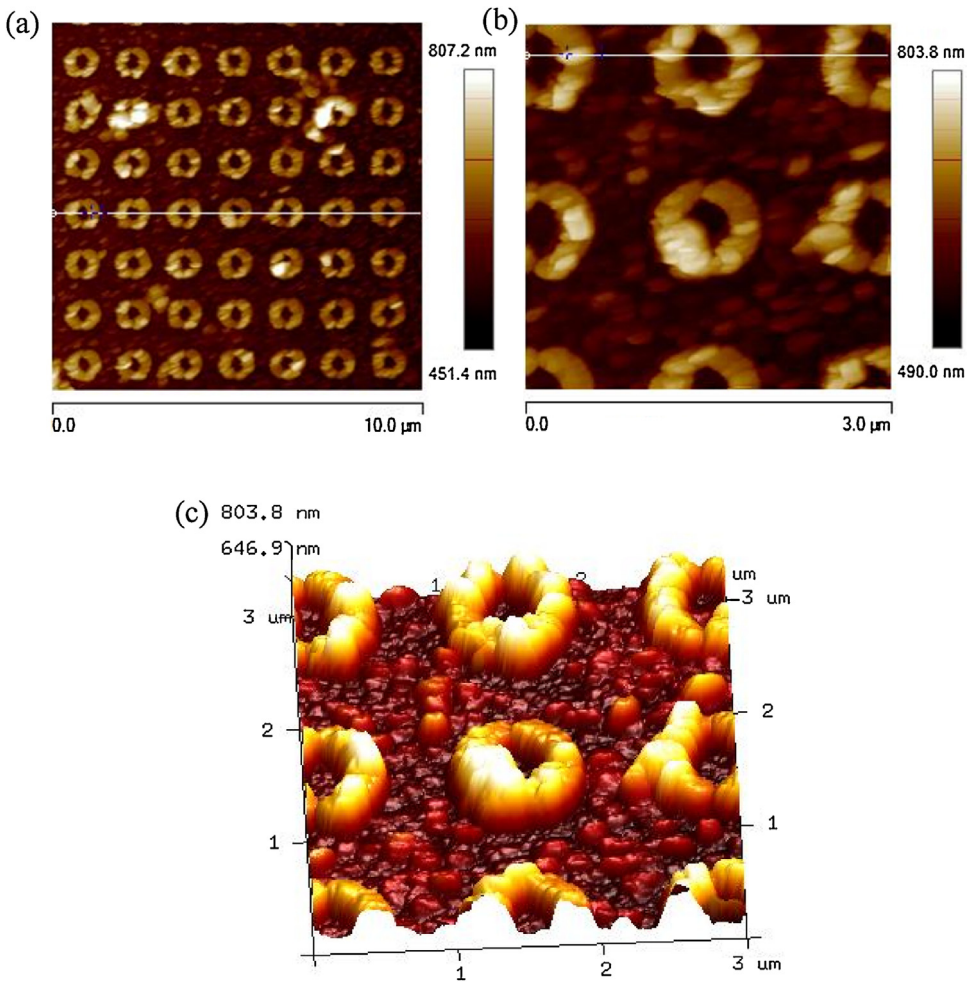

Fig. 7. (a) 2-D AFM images showing the deposition nature of 2.5 mM solution concentration of ODT molecular-films on the 730 nm diameter A-SRR array surfaces over an area of 10×10 μm^2, (b) closer view of the same part of the array over an area of 3×3 μm^2 with 3-D image shown in (c) respectively.

shown in Fig. 8(b) and (c) respectively. Based on the cross-sectional profiles, the minimum deposited thicknesses of the multilayer-films of ODT molecules on the ASRR array surfaces, obtained from a 2.5 mM solution concentration, are estimated to be approximately 17 nm, but with a maximum crystallised region height of approximately 92 nm. The similar deposition nature of the films is shown by the AFM images on the 710 and 750 nm diameter A-SRR array surfaces, which are shown in the supporting document in Fig. S2(a)–(d) respectively. The nature of the formation process for ODT thin-films on the ASRR array surfaces that has been observed in the present work differs from that of the targeted deposition and patterning of PMMA analyte on SRR surfaces, as described by Sharp et al. [33].

3.2. Non-resonant coupling

To compare the resonant-coupling with non-resonant coupling, further experiments were performed using a 2.5 mM ODT solution concentration in ethanol, with an identical immersion time of 3 h but using larger element diameter (1180 nm) A-SRR arrays. The resonance peaks appearing at wavelength of approximately 6 to 7 μm are far away from the CH_2 stretching vibrations of the ODT molecules. Comparison between the experimental and simulated transmittance responses from the 1180 nm diameter A-SRR array are shown in the supporting document in Fig. S3. The FTIR spectroscopic results for the adsorbed 2.5 mM solution concentration of the ODT-films on nanoantenna array surface, over an area of 300×300 μm^2, is shown in Fig. 9(a) - over the spectral region from 3 to 10 μm. The position of the ODT peaks are indicated by the dotted lines displaced vertically with respect to the ODT molecules -loaded spectrum. The ODT molecules related vibrational features are only visible when the spectra are magnified over the 3.3 to 3.6 μm wavelength region, as shown in the inset of the same Fig. 9(a). For the non-resonant coupling in Fig. 9(a), the change in amplitude of the ODT vibrational peaks is approximately six times smaller for a wavelength at 3.42 μm and approximately nine times smaller for the 3.5 μm vibrational peak - as compared with those for the resonant-coupling condition (see Fig. 5(b) and also in the supporting document in Fig. S1(a) and (b)), for the same immersion time of 3 h. Fig. 9(b) shows the 2-D AFM image of the 2.5 mM solution concentration of ODT molecules deposited on the 1180 nm diameter array surfaces over an area of 10×10 μm^2. The auto-generated scan profile obtained during the build-up of the AFM image (in Fig. 9(b)) is shown in Fig. 9(c), where the non-uniformity in the adsorbed film-thicknesses is clearly visible. Furthermore, the inhomogeneous and multilayer deposition nature of the ODT-films on the non-resonant A-SRR array surfaces is similar in nature to that of the resonant nanoantenna array surfaces - as shown in Fig. 7(a) and also in the supporting document in Fig. S2(a) and (b). Based on the AFM image in Fig. 9(b), the height profiles of cross-sections of the image are shown in the supporting document in Fig. S4(a)–(d) respectively. Based on the height profiles, the minimum and maximum deposited multilayer-film thicknesses are estimated to be approximately 17 nm and 92 nm respectively.

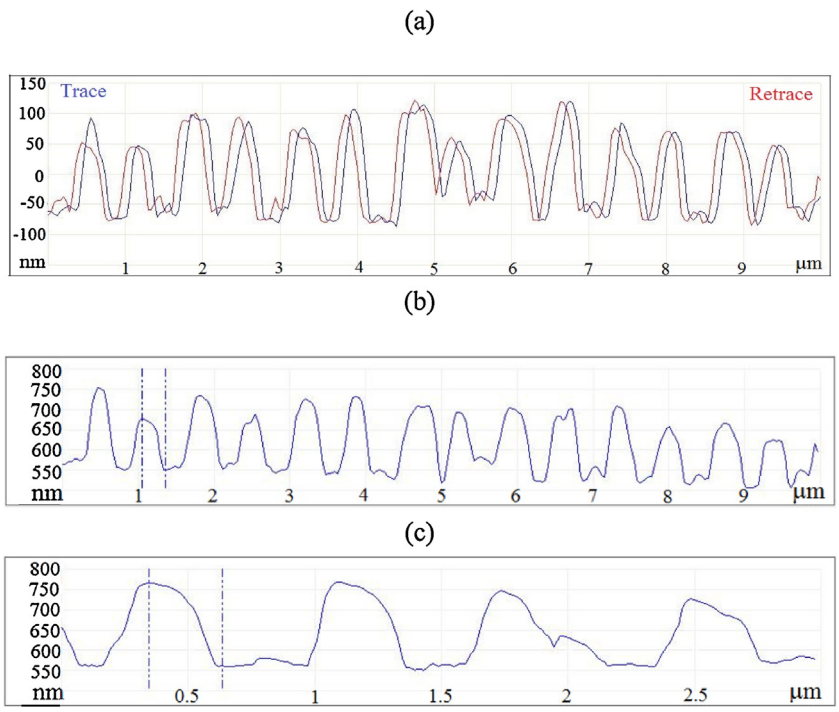

Fig. 8. (a) Graphics of the scan profile during the build-up of the AFM image in Fig. 7(a). (b) and (c): Height profiles of cross-sections of the images in Fig. 7(a) and (b) respectively.

Table 2
An estimation of the thicknesses and amplitudes of vibrational peak of the deposited ODT molecular-films on A-SRR array surfaces for different experimental conditions.

A-SRR outer diameter (nm)	Solutions concentration	Immersion Times (hours)	Deposited-film Thicknesses (nm)	Amplitude (%) (3.5 μm)
730	1 μM	24	2.34	0.095 (Fig. 2)
730	2.5 mM	3	17 (min) – 92 (max)	0.89 (Fig. 5(b))
1180	2.5 mM	3	17 (min) – 92 (max)	0.107 (Fig. 9(a))

Estimated ODT molecular-film thicknesses deposited for different solution concentrations and immersion times - together with the amplitudes of the vibrational peak at 3.5 μm - are given in Table 2. Based on these estimates, we conclude that the most dense and crystallised deposition of the ODT-films on the A-SRR array surfaces occurred for the 2.5 mM ODT solution concentration (when immersed for only 3 h) - in comparison with the monolayer-film obtained from the 1 μM solution concentration, for an immersion time of 24 h.

4. Discussion

Based on the two different solutions concentration of 2.5 mM and 1 μM of ODT molecules in ethanol, the AFM images show that - for the dilute, 1 μM ODT solution concentration, the formation of a well-ordered monolayer-film on the A-SRR array surfaces has occurred - with a calculated average film thickness of 2.34 nm, for the immersion time of 24 h. Whereas, deposition from the 2.5 mM ODT solution concentration, with a 3 h immersion time, led to the formation of dense, non-uniform multilayer ODT-films on the A-SRR array surfaces, together with some molecular assemblies, non-uniformly distributed over the substrate surface (see Fig. 7(a)–(c) and also in the supporting document Fig. S2(a)–(d) for resonant-coupling and Fig. S4(a)–(d) for non-resonant coupling). For the deposition of ODT molecules from a 2.5 mM solution concentration, the estimated minimum and maximum film thicknesses of between 17 nm to 92 nm, indicate highly the formation of inhomogeneous and non-uniform multilayer films on the nanoantenna array surfaces. Our findings disagree with the assumed monolayer-formation of 2.4 nm thick ODT-film deposited uniformly onto the resonator array surfaces, using the 2.5 mM ODT solution, as reported by Cubukcu et al. [15]. However, Neubrech et al. [9] had previously reported, from the deposition of 1 mM ODT solution onto gold nanoantenna array surfaces and using the resonant coupling condition, that 100 nm thickness of ODT layers were required to cover the nanoantenna array surfaces to match the theoretical simulation with their experimental results, thereby clearly showing multilayer ODT films formation for a millimolar (1 mM) ODT solution. Additionally, Kim et al. [19] have reported an estimated average thicknesses of the adsorbed ODT-films of 20 nm - on nanodisk array surfaces for the deposition from 1 mM ODT solution in ethanol for 24 h. These ODT molecules were non-uniformly assembled on the resonator surfaces, together with some molecular-assemblies spreading over the surface of the silicon (Si) substrate. These findings [9,19] are in accord with our findings for the millimolar (2.5 mM) solution concentration of ODT molecules.

Furthermore, the FTIR spectroscopy results represent the specific molecular vibrational responses related to the adsorbed thicknesses of the film formed on the resonator surfaces, for the different experimental conditions used. For resonant-coupling condition, the 2.5 mM solution concentration ODT molecular vibrational signals were detected most strongly (see Fig. 5(b) and Fig. S1(a) and (b) in the supporting document) - due to the dense and multilayer formation of films on the resonator surfaces. This result was supported by the AFM imaging (see Fig. 7 and Fig. S2 in the supporting document), albeit immersion was only for 3 h. In contrast, the symmetric CH_2 vibrational signal from the dilute, 1 μM solution concentration deposited ODT monolayer-film (immersion

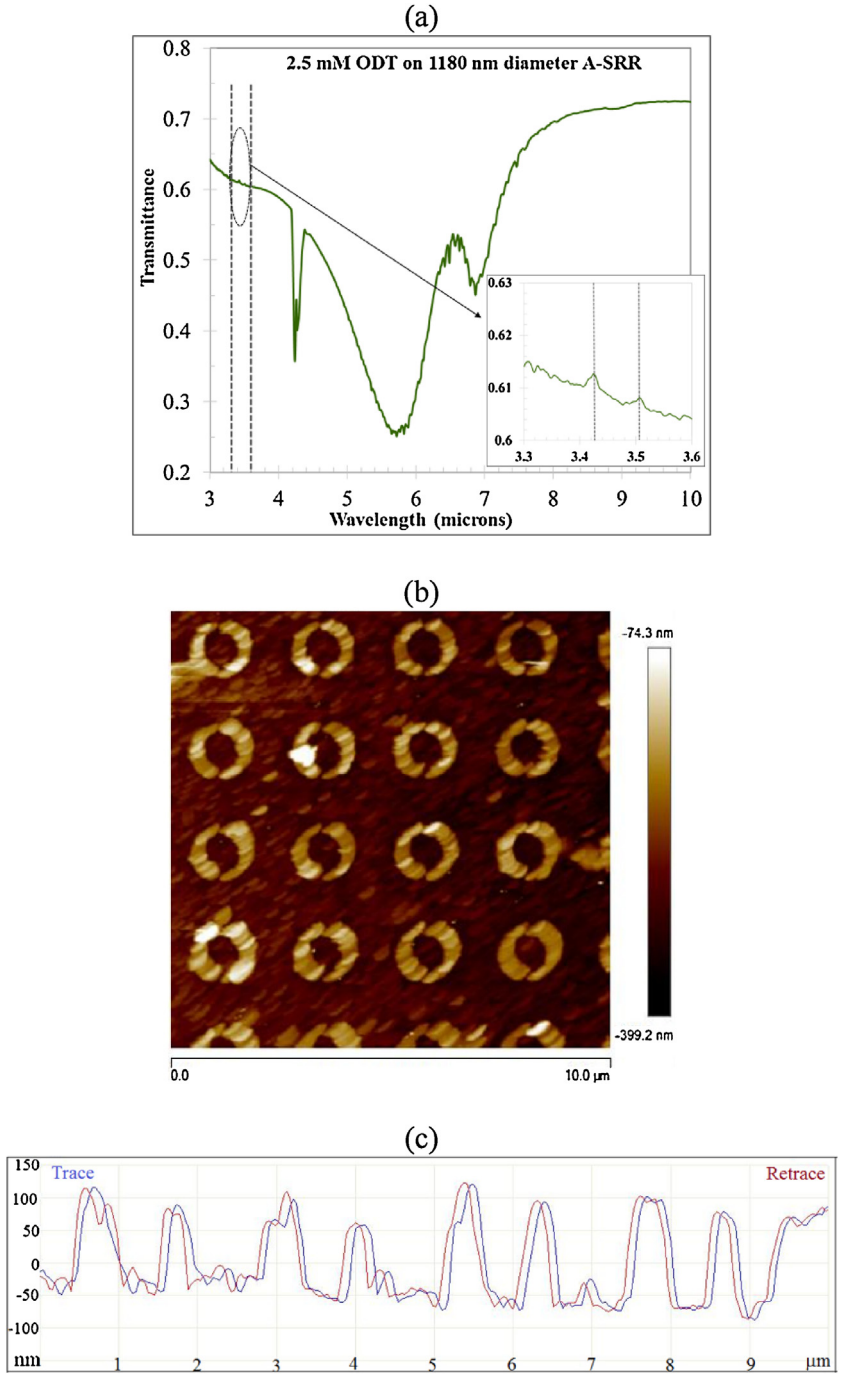

Fig. 9. (a): Transmittance spectra of the deposited 2.5 mM ODT solution molecular-films on the 1180 nm diameter ASRR array surfaces. The inset shows the magnified spectra of both ODT vibrational peaks over the 3.3–3.6 μm spectral region. (b) 2-D AFM image showing the deposition nature of 2.5 mM ODT molecular-films on the 1180 nm diameter A-SRR array surfaces. (c) Graphics of the scan-profile during the build-up of the AFM image in Fig. 9(b).

time of 24 h) only became clearly prominent when the spectra were magnified over the limited wavelength region from 3.3 to 3.6 μm (see Fig. 2). The number of molecules excited for the formation of monolayer ODT-film on A-SRR array surfaces is summarised in Table 1. For the 2.5 mM solution concentration, the molecular vibrational signal is approximately an order of magnitude larger for the resonant-coupling (see Fig. 5(b) and also in the supporting document Fig. S1(a) and (b)), as compared with the signal for the non-resonant coupling conditions (see Fig. 9(a)).

Estimated thicknesses of the deposited ODT molecular-films, together with the amplitudes of the vibrational peak at 3.5 μm for different experimental conditions, are summarised in Table 2. The amplitudes of the vibrational peaks (see Figs. 2, 5(b) and 9(a)) correlate with the estimated thicknesses of the deposited-films and are supported by the traces of the AFM images shown in Figs. 4(a), 8(b) and (c) - and in the supporting document in Fig. S4(c) and (d) respectively. With the same continuous self-assembled molecular deposition process, we have demonstrated the formation of a monolayer-film for the dilute, micromolar (1 μM) solution concentration, with a 24 h immersion time – whereas, multilayer films deposition was evident for the concentrated millimolar (2.5 mM) solution concentration, with only 3 h immersion. This result is due

to the kinetics of the molecular self-assembly process depending mainly on the solution concentrations - and is in accord with other findings reported in the literature [5,6].

We have chosen a 24 h immersion time for deposition of the 1 μM solution concentration ODT film on the gold A-SRR array surfaces - following Ishida et al. [35], where the continuous formation of self-assembled ODT-films on planar gold substrates was found to be independent of the substrate pre-treatment conditions for this longer immersion time. The deposited multilayer ODT-films, in our case, on the patterned plasmonic nanoantenna array surfaces in the present work [36] - and also on continuous unpatterned planar-gold surfaces [5] - are found to be stable for a long time (over several months). This property makes such nanoantenna arrays a versatile supporting platform for further binding experiments on biomolecules in their native biological environment [3] - or in electronics industry applications [37], where a high density of assembled-molecules is required for the creation of electronic components. We have realised the plasmonic nanoantennas on high refractive index (∼ 2.43 at 5.8 μm wavelength) [34] and transparent ZnSe substrates because ZnSe is highly transparent throughout the near to mid-IR spectral region. The plasmonic resonances of the engineered nanoantenna with larger diameters A-SRR array inscribed on ZnSe substrates are significantly red-shifted within the mid-IR spectral region (as shown in Fig. 9(a)), where the vibrational background of the protein molecules appears, which is of interest for future work. Other relevant possible application areas are in cell-culture research, bio-medical engineering and environmental sensing etc.

5. Conclusions

To our knowledge, we have imaged, for the first time, both monolayer and multilayer deposition of the ODT-films on the A-SRR array surfaces corresponding to different ODT solution concentrations and immersion times. The estimated film-thicknesses correlate with the amplitude of the molecular resonance peaks, based on surface enhanced infrared absorption (SEIRA) spectroscopy - and these estimates are also supported by the AFM traces. The use of resonant structures allow an increase in sensitivity with an order of magnitude over the non-resonant structures, under identical experimental conditions. The plasmonic resonant-coupling technique has enabled us to detect the monolayer ODT-film adsorbed on the resonator array surfaces after prolonged immersion in a dilute, micromolar (1 μM) solution concentration – which is three orders of magnitude lower in concentration than previously reported [9,15,16,18,19,23] and with attomole sensitivity of deposited material per A-SRR. Additionally, multilayer deposition of ODT-films were identified using the higher, millimolar (2.5 mM solution concentration) with a short immersion time.

Funding

Jharna Paul acknowledges the Daphne Jackson Trust (DJT) for providing her with a Fellowship, together with partial support by the Engineering and Physical Research Council (EPSRC) Grant (ref: EP/P51133X/1), to overcome the effects of a career gap to continue research and development in the field of science and engineering.

Acknowledgements

We acknowledge the facilities and the staff of the James Watt Nanofabrication Centre (JWNC) at the University of Glasgow for the provision of nano-fabrication and imaging.

Appendix A. Supplementary data

Supplementary material related to this article can be found, in the online version, at doi: https://doi.org/10.1016/j.sna.2018.05.032.

References

[1] R. Adato, A.A. Yanik, J.J. Amsden, D.L. Kaplan, F.G. Omenetto, M.K. Hong, S. Erramilli, H. Altug, Ultra-sensitive vibrational spectroscopy of protein monolayers with plasmonic nanoantenna arrays, Proc. Natl. Acad. Sci. U. S. A. 106 (2009) 19227–19232.
[2] C. Wu, A.B. Khanikaev, R. Adato, N. Arju, A.A. Yanik, H. Altug, G. Shvets, Fano-resonant asymmetric metamaterials for ultrasensitive spectroscopy and identification of molecular monolayers, Nat. Matt. 11 (2012) 69–75.
[3] R. Adato, H. Altug, *In-situ* ultra-sensitive infrared absorption spectroscopy of biomolecule interactions in real time with plasmonic nanoantennas, Nat. Commun. 4 (2154) (2013) 1–10.
[4] G.A. Hudalla, W.L. Murphy, Chemically well-defined self-assembled monolayers for cell culture: toward mimicking the natural ECM, Soft Matter 7 (2011) 9561–9571.
[5] C.D. Bain, E.B. Troughton, Yu-T. Tao, J. Evall, G.M. Whitesides, R.G. Nuzzo, Formation of monolayer films by the spontaneous assembly of organic thiols from solution onto gold, J. Am. Chem. Soc. 111 (1989) 321–335.
[6] K.A. Peterlinz, R. Georgiadis, In situ kinetics of self-assembly by surface plasmon resonance spectroscopy, Langmuir 12 (1996) 4731–4740.
[7] Yeon-T. Kim, R.L. McCarley, A.J. Bard, Observation of *n*-octadecanethiol multilayer formation from solution onto gold, Langmuir 9 (1993) 1941–1944.
[8] F. Bensebaa, R. Voicu, L. Huron, T.H. Ellis, E. Kruus, Kinetics of formation of long-chain *n*-alkanethiolate monolayers on polycrystalline gold, Langmuir 13 (1997) 5335–5340.
[9] F. Neubrech, A. Pucci, T.W. Cornelius, S. Karim, A. García-Etxarri, J. Aizpurua, Resonant plasmonic and vibrational coupling in a tailored nanoantenna for infrared detection, Phys. Rev. Lett. 101 (2008), 157403-1-4.
[10] C.A. Alves, E.L. Smith, M.D. Porter, Atomic scale imaging of alkanethiolate monolayers at gold surfaces with atomic force microscopy, J. Am. Chem. Soc. 114 (1992) 1222–1227.
[11] R.L. McCarley, D.J. Dunaway, R.J. Willicut, Mobility of the alkanethiol-gold (111) interface studied by scanning probe microscopy, Langmuir 9 (1993) 2775–2777.
[12] K.B. Crozier, A. Sundaramurthy, G.S. Kino, C.F. Quate, Optical antennas: resonators for local field enhancement, J. Appl. Phys. 94 (2003) 4632–4642.
[13] P. Mühlschlegel, H.-J. Eisler, O.J.F. Martin, B. Hecht, D.W. Pohl, Resonant optical antennas, Science 308 (2005) 1607–1609.
[14] V. Giannini, A.I. Fernández-Domínguez, Y. Sonnefraud, T. Roschuk, R. Fernández-García, S.A. Maier, Controlling light localization and light-matter interactions with nanoplasmonics, Small 6 (2010) 2498–2507.
[15] E. Cubukcu, S. Zhang, Yong-S. Park, G. Bartal, X. Zhang, Split ring resonator sensors for infrared detection of single molecular monolayers, Appl. Phys. Lett. 95 (2009), 043113-1-3.
[16] L.V. Brown, K. Zhao, N. King, H. Sobhani, P. Nordlander, N.J. Halas, Surface-enhanced infrared absorption using individual cross antennas tailored to chemical moieties, J. Am. Chem. Soc. 135 (2013) 3688–3695.
[17] C. Huck, F. Neubrech, J. Vogt, A. Toma, D. Gerbert, J. Katzmann, T. Härtling, A. Pucci, Surface- enhanced infrared spectroscopy using nanometer-sized gaps, ACS Nano 8 (2014) 4908–4914.
[18] C. Huck, A. Toma, F. Neubrech, M. Chirumamilla, J. Vogt, F. De Angelis, A.M. Pucci, Gold nanoantennas on a pedestal for plasmonic enhancement in the infrared, ACS Photon. 2 (2015) 497–505.
[19] J. Kim, A. Dutta, B. Memarzadeh, A.V. Kildishev, H. Mosallaei, A. Boltasseva, Zinc oxide based plasmonic multilayer resonator: localized and gap surface plasmon in the infrared, ACS Photon. 2 (2015) 1224–1230.
[20] I.G. Mbomson, S. Tabor, B. Lahiri, G. Sharp, S.G. McMeekin, R.M. De La Rue, N.P. Johnson, Asymmetric split H-shape nanoantennas for molecular sensing, Biomed. Opt. Exp. 8 (January) (2017) 395–406.
[21] A.G. Milekhin, O. Cherkasova, S.A. Kuznetsov, I.A. Milekhin, E.E. Rodyakina, A.V. Latyshev, S. Banerjee, G. Salvan, D.R.T. Zahn, Nanoantenna-assisted plasmonic enhancement of IR absorption of vibrational modes of organic molecules, Beilstein J. Nanotechnol. 8 (May) (2017) 975–981.
[22] F. Kusa, I. Morichika, A. Takegami, S. Ashihara, Enhanced ultrafast infrared spectroscopy using coupled nanoantenna arrays, Opt. Exp. 25 (May) (2017) 12896–12907.
[23] X. Chen, Chu Wang, Y. Yao, Chao Wang, Plasmonic vertically coupled complementary antennas for dual-mode infrared molecule sensing, ACS Nano 11 (July) (2017) 8034–8046.
[24] L. Dong, X. Yang, C. Zhang, B. Cerjan, L. Zhou, M.L. Tseng, Y. Zhang, A. Alabastri, P. Nordlander, N.J. Halas, Nanogapped Au antennas for ultrasensitive surface-enhanced infrared absorption spectroscopy, Nano Lett. 17 (August) (2017) 5768–5774.
[25] T.H.H. Le, T. Tanaka, Plasmonics-nanofluidics hybrid metamaterial: an ultrasensitive platform for infrared absorption spectroscopy and quantitative measurement of molecules, ACS Nano 11 (September) (2017) 9780–9788.

[26] M. Xi, B.M. Reinhard, Localized surface plasmon coupling between mid-IR-resonant ITO nanocrystals, J. Phys. Chem. C 122 (2018) 5698–5704.
[27] http://www.sigmaaldrich.com/catalog/product/sial/74731.
[28] D. Lin-Vien, N.B. Colthup, W.G. Fateley, J.G. Grasselli, The Handbook of Infrared and Raman Characteristic Frequencies of Organic Molecules, 1st ed., Academic Press, 1991, ISBN: 978-0-12-451160-6.
[29] V.A. Fedotov, M. Rose, S.L. Prosvirnin, N. Papasimakis, N.I. Zheludev, Sharp trapped-mode resonances in planar metamaterials with a broken structural symmetry, Phys. Rev. Lett. 99 (2007) 147401–147404.
[30] K. Aydin, I.M. Pryce, H.A. Atwater, Symmetry breaking and strong coupling in planar optical metamaterials, Opt. Exp. 18 (2010) 13407–13417.
[31] B. Lahiri, A.Z. Khokhar, R.M. De La Rue, S.G. McMeekin, N.P. Johnson, Asymmetric split ring resonators for optical sensing of organic materials, Opt. Exp. 17 (2009) 1107–1115.
[32] B. Lahiri, S.G. McMeekin, R.M. De La Rue, N.P. Johnson, Resonance hybridization in nanoantenna arrays based on asymmetric split-ring resonators, Appl. Phys. Lett. 98 (2011), 153116-1-3.
[33] G.J. Sharp, H. Vilhena, B. Lahiri, S.G. McMeekin, R.M. De La Rue, N.P. Johnson, Mapping the sensitivity of split ring resonators using a localized analyte, Appl. Phys. Lett. 108 (2016), 251105-1-5.
[34] https://www.crystran.co.uk/optical-materials/zinc-selenide-znse.
[35] T. Ishida, S. Tsuneda, N. Nishida, M. Hara, H. Sasabe, W. Knoll, Surface-conditioning effect of gold substrates on octadecanethiol self-assembled monolayer growth, Langmuir 13 (1997) 4638–4643.
[36] J. Paul, S.G. McMeekin, R.M. De La Rue, N.P. Johnson, Deposition of organic molecules on gold nanoantennas for sensing, in: Proc. SPIE 10227, SPIE Optics and Optoelectronics: Metamaterials XI, Czech Republic, Prague, 2017, http://dx.doi.org/10.1117/12.2269937, 10227Z-1-8.
[37] L. Newton, T. Slater, N. Clark, A. Vijayaraghavan, Selfassembled monolayers (SAMs) on metallic surfaces (gold and graphene) for electronic applications, J. Mater. Chem. C 1 (2013) 376–393.

Biographies

Jharna Paul (Former surname: Mandal) is a Research Associate within the Quantum Sensors Group at The University of Glasgow where her research focuses on the design and fabrication of integrated photonic circuits for quantum computing and sensing applications. In 2014, Jharna was awarded with a part-time Daphne Jackson Trust Fellowship (to overcome her long career-gap) and researched on the growth of organic-thin films for bio-molecular sensing applications. She received her BEng and PhD degrees from The Regional Engineering College, Trichy, India in 1997 and The City University, London in 2006 respectively. She has published more than 25 papers in both Journals and Conferences.

Scott McMeekin is a Professor in the School of Engineering and Built Environment at Glasgow Caledonian University. He received a BSc degree from The University of Strathclyde in 1985 and the MSc and PhD degrees from The University of Glasgow in 1986 and 1989 respectively. His current research interests include the development of Instrumentation and Sensor Systems with a specific interest in the condition monitoring of energy assets and the development of photonic bio-sensors. He has published over 130 journal and conferences articles and is co-inventor on 6 patents.

Richard De La Rue's research has been concerned with photonic crystal and photonic wire structures, waveguide micro-cavities, silicon photonics, metamaterials and graphene (oxide) photonics. His work has also included research on compact lasers, photonic-crystal LEDs and the applications of photonic crystal structures and metamaterial surfaces to bio-medical and organic sensing. He has published more than 290 articles as papers in journals, magazines and book chapters. He is a Fellow of a) European Optical Society, b) Optical Society of America, c) IEEE, d) Royal Academy of Engineering, e) Royal Society of Edinburgh and f) IET. His Google Scholar h-index is currently 57.

Dr Nigel P. Johnson is a former Reader and now Honorary Research Fellow in the School of Engineering at The University of Glasgow. He received BSc and MSc degrees from The University of Manchester in 1980 and 1982 and a PhD degree from The University of Strathclyde in 1986. His research interests include Photonic Crystals, Metamaterials and both Chemical and Biosensors. He has published over 190 journal and conference articles, and is Fellow of IoP, IET and SPIE.